Internet of Things 36 (2026) 101862

Contents lists available at ScienceDirect

Internet of Things

journal homepage: www.elsevier.com/locate/iot

Neuromorphic solar edge AI for sustainable wildfire detection

Raúl Parada *

Centre Tecnològic de Telecomunicacions de Catalunya (CTTC/CERCA), Castelldefels, 08860, Catalonia, Spain

ARTICLE INFO

Keywords:
Edge AI
Neuromorphic computing
Solar-Powered drones
Wildfire detection
Internet of robotic things
Sustainable monitoring

ABSTRACT

This paper presents a feasibility study of a solar-autonomous wildfire detection system using neuromorphic edge AI on fixed-wing drones. Through a comprehensive year-long simulation over Parc del Garraf (Catalonia), we evaluate three edge computing platforms, Raspberry Pi 4, Google Coral TPU, and BrainChip Akida, integrated into solar-optimized eBee X drones. Results show that the BrainChip Akida achieves 4200 patrol hrs per yr, nearly three times that of traditional CPU systems, while maintaining 87 % solar energy autonomy. The Google Coral TPU and Raspberry Pi 4 reach 66 % and 52 % autonomy, respectively. Fleet scaling analysis demonstrates that increasing drone count from one to eight reduces median wildfire detection time from 18 to 2.2 hrs, surpassing critical response thresholds. Seasonal analysis reveals Akida-based systems can operate fully on solar energy during summer and most of spring and fall, minimizing grid dependency. These findings establish neuromorphic computing as a foundational technology for sustainable, perpetual environmental monitoring within the Internet of Robotic Things (IoRT).

1. Introduction

Wildfires are now responsible for billions of dollars in annual economic losses and hundreds of lives globally. In the Mediterranean basin, over 500,000 hectares are burned yearly, often with delayed detection times exceeding 12 hrs. These delays critically hinder suppression efforts and exacerbate damage. As climate change intensifies droughts and heatwaves, the urgency for faster, autonomous detection systems grows [1]. Mediterranean ecosystems, in particular, face growing risk as traditional fire detection systems, relying on satellite imagery, human patrols, or fixed ground sensors, struggle with temporal latency, limited spatial coverage, and infrastructure dependency. Other proposals incorporate artificial intelligence (AI) and fifth generation (5G) for wildfire control [2], but such approaches still rely heavily on communication infrastructure.

Recent advances in unmanned aerial vehicles (UAVs) have opened new possibilities for continuous, real-time environmental monitoring. However, most current drone-based detection systems are hindered by significant energy limitations, requiring frequent manual recharging or access to grid-based infrastructure. This severely restricts their autonomy and scalability, especially in remote or high-risk natural environments where rapid response is critical.

The Internet of robotic things (IoRT) envisions fully autonomous, intelligent agents operating over long durations without human intervention. Achieving this vision in the context of wildfire monitoring demands breakthroughs in two main areas: (i) onboard decision-making through efficient Edge AI [3], and (ii) self-sustaining energy systems. While Edge AI reduces reliance on cloud connectivity and improves latency, traditional computing platforms such as CPUs or even typical TPUs consume too much power for extended operation. As such, they cannot meet the demands of uninterrupted surveillance missions without significant energy support.

* Corresponding author.
E-mail address: rparada@cttc.es

https://doi.org/10.1016/j.iot.2025.101862
Received 27 September 2025; Received in revised form 28 November 2025; Accepted 22 December 2025
Available online 29 December 2025

Neuromorphic computing offers a compelling solution. By mimicking the efficiency of biological brains [4], neuromorphic processors such as BrainChip Akida enable ultra-low-power inference, operating at a fraction of the energy cost of conventional architectures. Coupled with solar energy harvesting, this opens the door to continuous aerial monitoring, without external energy input, for the first time to the best of our knowledge.

This work addresses the critical challenge of enabling truly autonomous environmental monitoring drones by combining neuromorphic Edge AI and solar energy systems. The core objectives of our study are:

1. To quantify and compare the energy sustainability potential of neuromorphic and traditional edge computing platforms when deployed on UAVs in realistic wildfire surveillance scenarios.
2. To simulate year-round operations using real solar irradiance and environmental data, modelling energy harvesting and consumption dynamics in detail.
3. To establish practical benchmarks for operational availability, solar autonomy, and wildfire detection performance across different hardware configurations.

The rest of this paper is structured as follows: Section 2 reviews related work in UAV-based wildfire detection and sustainable edge AI. Section 3 details the simulation framework, hardware platforms, energy modeling, and fleet scaling strategies. Section 4 presents and analyzes the simulation results, including mission time allocation, solar autonomy, seasonal variations, and cost-effectiveness. Section 5 discusses the broader implications of these results for sustainable IoRT systems. Finally, Section 6 concludes the paper and outlines future research directions.

2. Related work

Recent years have witnessed significant progress in UAV-based wildfire detection, AI-enabled edge processing, and neuromorphic computing for environmental monitoring. Here, we provide a structured comparison of leading approaches and clarify the main research gaps that remain.

2.1. UAV-based wildfire detection and mitigation systems

A broad class of solutions leverages fleets of UAVs for fire mapping, real-time perimeter tracking, and early response. Bailon-Ruiz et al. [5] introduced a fleet-based wildfire monitoring framework, integrating fire propagation simulation with collaborative trajectory planning via Variable Neighborhood Search. Their system, validated in simulation and field trials, delivers adaptive, near real-time fire mapping, but relies on manual or centralized coordination and general-purpose UAV CPUs. John et al. [6] presented the CREDS framework, a decentralized, auction-based planner enabling robust sequential UAV assignments for fire detection and mitigation under partial observability. CREDS achieves high scalability and rapid response even when fires vastly outnumber UAVs, by treating fires as dynamically growing tasks with deadlines and using consensus-based coordination. Most prior platforms focus on either detection or mapping without modeling onboard energy sustainability or integrating full-stack autonomy.

2.2. AI and edge AI approaches

Embedded AI at the UAV edge enables local inference, latency reduction, and independence from cloud connectivity. Ramadan et al. [7] developed a scalable UAV-IoT system that integrates distributed LoRa-based sensor nodes, AI-enabled drones for fire detection/tracking, and a cloud backend for reporting and mission dispatch. Their approach demonstrates high detection accuracy (>99 %) and low response times (<5min), using low-cost hardware and a modular AI pipeline. Carrillo et al. [8] advanced the paradigm by running high-resolution wildfire spread simulations in situ on edge GPU modules (Nvidia Jetson), rather than on remote HPC/cloud. This reduces operational latency and makes feasible real-time prediction even in areas with low network coverage, though the energy consumption of these GPU platforms still constrains long-duration field operation.

2.3. Neuromorphic platforms and spiking neural networks

Energy efficiency and perpetual autonomy are possible using neuromorphic hardware, which supports SNNs for event-based perception and ultra-efficient compute. Lundin and Winzell [9] demonstrated a UAV detection system using event cameras and SNNs on the SynSense Speck SoC, with deployment power below 7mW and year-long operation from a battery, a massive improvement over standard GPU-based approaches. Paredes-Vallés et al. [10] implemented a fully neuromorphic flight control pipeline on Intel's Loihi, encompassing both perception (from event cameras) and onboard control inference (hovering, landing, maneuvering) at 200Hz, with real drone validation. Sanyal et al. [11] proposed a physics-guided, neuromorphic navigation framework that ties event-driven perception from DVS to energy-aware path planning using spiking neural nets and lightweight neural models, supporting robust, low-latency navigation in dynamic environments. Beyond system-level neuromorphic platforms, recent advances in memristive synaptic devices are enabling next-generation ultra-low-power neuromorphic hardware. Miao et al. demonstrated tantalum oxide-based synaptic transistors with femtojoule-level switching energy for efficient SNN implementations [12]. Fan et al. reviewed emerging nanomaterials for neuromorphic computing, highlighting 2D materials and oxide heterostructures that promise orders-of-magnitude efficiency improvements over current CMOS-based neuromorphic chips [13]. Wan et al. provided a comprehensive survey of neuromorphic devices

Table 1
Comparison of UAV wildfire detection and response systems by approach, hardware, coordination sophistication, and highlights.

Reference	Year	Application	Platform/AI	Highlights
Bailon-Ruiz et al.	2022	Multi-UAV mapping	Onboard CPU	Cent. VNS; minimal mapping energy cost; no energy model; single mission validated
John et al.	2020	Wildfire mitigation	Not specified	Decentralised, deadline-prioritised (CRUES); scalable (41 UAVs); fire growth modes; no energy constraints
Ramadan et al.	2024	UAV-IoT detect/track	Edge CPU + IoT	Auto. UAV; IoT-centric; hybrid ALT + IoT dispatch; high accuracy agents
Carrillo et al.	2025	Fire spread sim.	Jetson GPU	Single-node sim.; energy-aware mission; UAV integration; battery-centric
Lundin & Wimmell	2022	Low-power detection	Speck SNN (7 μW)	Local perception; ultra-low power; onboard SNN processing; long-term operation
Paredes-Vallés et al.	2024	End-to-end SNN	Loihi 19 (30 μW)	Neuromorphic SNN; end-to-end learning; energy-efficient (30 μW); UAV agent
Sanyal et al.	2025	Energy-eff. nav.	Loihi, SNN	Physics-guided SNN; energy saving; neuromorphic; DVS-based
Our work	2025	**Solar-auton. fleet detect.**	**RPi4, Coral, Akida, solar UAV**	**Solar-powered neuromorphic fleet; high autonomy; long patrol; ecosystem; decentralized-ready; year-long multi-UAV sim; solar/hardware integrated**

and algorithms, emphasizing the co-design opportunities between device physics and network architectures for edge AI applications [14]. These hardware advances complement algorithmic developments and suggest that future UAV platforms could achieve even lower power consumption than the BrainChip Akida evaluated in this study.

2.4. Summary comparison

Table 1 offers a comparative overview of these pivotal studies, with columns detailing application focus, hardware and AI platform, coordination or planning model, and the principal contributions or distinguishing features of each approach, including our own work's advances in solar-powered neuromorphic fleet autonomy and integrated year-scale simulation.

Despite broad advances, several gaps persist:

- *Energy sustainability*: Most UAV-based wildfire platforms do not model solar energy harvesting or simulate year-long field autonomy hampering sustainable or gridless deployment [8–10].
- *End-to-end neuromorphic integration*: While SNNs and event-based processing are validated for low-power perception and (single) UAV control, there is little research on real fleet-level or multi-UAV neuromorphic coordination [9,10].
- *Full-stack, Realistic validation*: Few solutions combine physics-based solar energy models, hardware power characterization, and scalable, landscape-level multi-UAV mission planning with empirical datasets.
- *Scalable, Decentralized swarm control*: Even robust decentralized planners like CREDS [6] have not yet been validated in solar-perpetual, neuromorphic, or fully autonomous fleet contexts.
- *Unified AI/IoT edge integration*: The co-design of fleet-wide autonomy, rapid decentralized detection, and grid-independent power is rare (prior systems are often modular, task-limited, or focus on detection/response in isolation).

This motivates the need for a solar-autonomous, neuromorphically enabled UAV fleet solution with year-scale, real-world simulation and scalable, energy-aware swarm coordination, as undertaken in our paper.

3. Methodology

This section presents the complete simulation methodology designed to evaluate the energy autonomy, detection capacity, and mission viability of solar-powered drones equipped with different edge AI platforms, including neuromorphic computing. The simulation is implemented using Python and is verifiable via the accompanying codebase. It models the performance of drones operating autonomously over a full year, incorporating solar harvesting dynamics, energy consumption profiles, patrol logic, and fleet scaling.

3.1. Simulation environment and geographic scope

The area of study is Parc del Garraf in Catalonia, Spain (latitude: 41.30°N, longitude: 1.90°E), a wildfire-prone Mediterranean ecosystem covering approximately 128 km^2. This region was selected due to its ecological relevance and variable seasonal solar availability. The simulation spans 365 days, modeling energy flows on a daily basis to capture inter-seasonal fluctuations in solar irradiance and fire risk. Solar radiation data was approximated using a smoothed sinusoidal model (RMSE = 14.3 Wh/day over 365 days) fitted to empirical values from the NASA POWER database. This model accurately reproduces daily solar input variations typical of the Mediterranean climate. The sinusoidal model was chosen over alternative approaches (polynomial fits, lookup tables, or complex radiative transfer models) for several reasons. First, it physically represents the astronomical solar declination cycle that dominates seasonal variation at the study latitude (41.3°N). Second, it provides computational efficiency for year-long simulations with minimal parameters while maintaining good agreement with NASA POWER empirical data (RMSE = 14.3 Wh/day, R^2 = 0.96). Third, the model parameters-mean irradiance (235 Wh/day), seasonal amplitude (150 Wh/day), and phase offset (80 days), have direct physical interpretations corresponding to annual average solar input, seasonal variation magnitude, and winter solstice alignment, respectively. This approach balances accuracy, computational tractability, and interpretability for comparative energy autonomy assessment.

3.2. Drone platform specification

The simulated drone platform is a modified *eBee X Solar* fixed-wing UAV by AgEagle, enhanced with lightweight photovoltaic modules. The drone's core power requirements are modeled as follows: 28 W of power during cruise flight (representing propulsion load), and 3 W dedicated to avionics subsystems (including GPS, communication, and flight control). The onboard battery has a capacity of 148 Wh, enabling a maximum continuous flight time of approximately 4.8 hrs when fully charged.

The solar array affixed to the drone consists of 0.20 m^2 of high-efficiency flexible panels with a nominal efficiency of 25 %. The theoretical peak solar output, assuming optimal irradiance, is 47.5 W. The average daily harvest was modeled to follow seasonal trends, with an annual mean of 235 Wh/day.

3.3. Edge AI hardware modeling

Three representative edge inference platforms were simulated, covering a spectrum of energy efficiency and computational power:

- **Raspberry Pi 4B (Pi 4):** A general-purpose CPU-based platform, consuming 6.0 W during inference and 3.0 W when idle. Its inference latency is approximately 200 ms [15].
- **Google Coral TPU (Coral):** An edge accelerator designed for AI workloads, requiring 2.0 W during inference and 1.6 W at idle, with an average latency of 12 ms [16].
- **BrainChip Akida (Akida):** A neuromorphic processor mimicking spiking neural networks, consuming only 0.30 W during inference and 0.15 W at idle. It offers an ultra-low inference latency of 10 ms [17].

These platforms were benchmarked based on official documentation and third-party empirical studies, ensuring realistic power and latency modeling.

3.3.1. Why spiking neural networks excel at wildfire detection

The BrainChip Akida's Spiking Neural Network (SNN) architecture achieves simultaneous low power consumption and low latency through three key mechanisms particularly suited to wildfire detection:

1. Event-driven computation:

Unlike conventional DNNs that process entire image frames at fixed intervals (e.g., 30 FPS), SNNs activate only when input features change significantly [18,19]. For aerial wildfire surveillance, where most frames contain uniform forest canopy, this sparse activation dramatically reduces computation. Only pixels exhibiting temporal changes (smoke plumes, flame reflections) trigger neuronal spikes, reducing active neuron count by 70–90 % compared to frame-based processing [20,21]. This translates directly to proportional power savings: inference power of 0.30W for Akida versus 6.0W for Pi4 CPU. Event-driven learning on neuromorphic hardware has demonstrated up to 30-fold reduction in energy consumption compared to time-step-based methods [18], and SNNs can achieve energy savings of up to 1000× when deployed on specialized neuromorphic hardware [20].

2. Temporal coding efficiency:

SNNs encode information in spike timing rather than activation magnitudes [22,23]. For wildfire signatures (flickering flames, rising smoke), temporal patterns are naturally captured without expensive recurrent memory structures. A smoke plume's characteristic upward drift or flame flicker (2–10 Hz) is encoded in spike intervals, enabling robust detection with ~10ms latency, critical for real-time UAV response while consuming minimal energy [22]. Temporal coding schemes allow SNNs to process sensory information based on the relative timing of spikes, achieving high accuracy with single-spike latencies [22,24]. This is particularly advantageous for detecting transient wildfire events where timing information is critical.

3. Neuromorphic memory integration:

Akida's on-chip SRAM is tightly coupled with spiking neuron arrays, eliminating off-chip memory access, a primary energy drain in conventional architectures [21,25]. Wildfire detection models (trained using CNN-to-SNN conversion on datasets like FLAME) fit

entirely on-chip (≈2MB model size), avoiding external DRAM and PCIe transfers that dominate Pi4/Coral energy budgets. Neuromorphic chips merge computation and memory within the same architecture, eliminating the von Neumann bottleneck and minimizing data transfer delays [25]. This co-location of memory and compute reduces energy consumption by up to 98 % in robotics applications, as demonstrated by IBM's TrueNorth chip in DARPA trials [21].

Application-specific advantage:

Wildfire detection inherently involves sparse events (fires occupy <0.1 % of surveillance area at any time) in quasi-static environments (slow forest scene changes), perfectly matching SNN's event-driven paradigm [19]. Conventional DNNs waste energy processing empty sky and unchanging terrain; SNNs activate only on fire-relevant features, achieving the demonstrated 87 % solar autonomy critical for perpetual monitoring. Neuromorphic architectures operate in an asynchronous, event-driven mode, activating only when meaningful changes occur, ideal for edge devices with intermittent activity patterns [25].

3.4. Solar energy harvest modeling

Solar input across the year was modeled using a sinusoidal approximation. The daily energy harvested on day d of the year is defined as $Harvest_{day} = 235 + 150 \cdot \sin\left(\frac{2\pi(d-80)}{365}\right)$ [Wh/day]. This equation captures the cyclical nature of solar irradiance, peaking in mid-summer and declining in winter. The peak corresponds to June-July (maximum solar altitude), while the trough falls around December-January.

The 13 % derating factor represents cumulative efficiency losses from multiple sources common in UAV-mounted photovoltaic systems. These include: (i) **temperature losses** (≈5 %), as panel efficiency degrades approximately 0.4–0.5 %/°C above standard test conditions (25°C) [26,27], and Mediterranean operational temperatures reach 35–40°C during peak solar hrs; (ii) **soiling and atmospheric losses** (≈3 %), from dust accumulation on panels during flight and atmospheric particulate scattering, which can reduce efficiency by 2–6 % in Mediterranean climates [28,29]; (iii) **DC wiring resistance** (≈2 %), from ohmic losses in cables connecting panels to charge controllers [30]; and (iv) **MPPT conversion losses** (≈3 %), from charge controller inefficiencies despite modern maximum power point tracking [31,32]. The compound effect is calculated as: $0.95 \times 0.97 \times 0.98 \times 0.97 \approx 0.87$, yielding the 13 % total loss factor. These values are consistent with photovoltaic system modeling standards [33] and are conservative for UAV applications where in-flight panel cleaning is impractical [34]. Thus, the final usable solar power $P_{\text{solar}}(t)$ at time t is computed as $P_{solar}(t) = GHI(t) \cdot A_{panel} \cdot \eta_{panel} \cdot \eta_{losses}$ where GHI(t) (global horizontal irradiance at time t), A_{panel} with value 0.20 m^2, η_{panel} with value 0.25 and η_{losses} as 0.87. The conversion from daily energy harvest (Wh/day) to instantaneous usable power (W) accounts for the temporal distribution of solar availability. The average usable power during daylight hrs is computed as:

$$P_{\text{solar,avg}} = \frac{E_{\text{harvest,day}} \times \eta_{\text{losses}}}{t_{\text{sunlight}}}$$

where $E_{\text{harvest,day}}$ is the daily harvested energy (Wh/day) from the sinusoidal model (Eq. in Section 3.1), $\eta_{\text{losses}} = 0.87$ is the combined system efficiency after derating (13 % total loss), t_{sunlight} is the effective sunlight hrs per day (seasonally variable: 4–6 hrs winter, 8–10 hrs summer), and $P_{\text{solar,avg}}$ is the average power available during charging periods (W). This approach follows the peak sun hrs methodology for PV system sizing [35,36].

For instantaneous modeling at time t, the usable power is:

$$P_{\text{solar}}(t) = \text{GHI}(t) \times A_{\text{panel}} \times \eta_{\text{panel}} \times \eta_{\text{losses}}$$

where GHI(t) is the global horizontal irradiance (W/m^2) [37], $A_{\text{panel}} = 0.20$ m^2 is the panel area, and $\eta_{\text{panel}} = 0.25$ is the nominal panel efficiency. This standard photovoltaic power model is widely used in solar UAV energy analysis [38,39].

3.5. Energy consumption modeling

The simulation assumes a daily operational cycle of 10 hrs of active patrol (during which the inference hardware operates continuously) and 14 hrs of idle or charging time. The total daily energy consumption is derived by summing the contributions from propulsion, avionics, and AI hardware during patrol, and idle draw during standby:

For the Raspberry Pi 4, the daily energy consumption is computed as $Energy_{day} = (28 + 3 + 6.0) \cdot 10 + (3.0) \cdot 14 = 412$ Wh/day.

Equivalent daily energy consumption calculations for the other platforms are:

Google Coral TPU:

$$E_{\text{day,Coral}} = (28 + 3 + 2.0) \times 10 + 1.6 \times 14 = 330 + 22.4 = 352.4 \text{ Wh/day} \quad (1)$$

comprising 330 Wh during active patrol (propulsion + avionics + TPU inference) and 22.4 Wh during idle/charging periods. The Google Coral Edge TPU achieves superior energy efficiency compared to CPU-based processing through dedicated neural network acceleration hardware [40,41].

BrainChip Akida:

$$E_{\text{day,Akida}} = (28 + 3 + 0.30) \times 10 + 0.15 \times 14 = 313 + 2.1 = 315.1 \text{ Wh/day} \quad (2)$$

comprising 313 Wh during patrol and only 2.1 Wh during idle, demonstrating the ultra-low power advantage of neuromorphic computing. The BrainChip Akida's event-driven spiking neural network architecture achieves orders-of-magnitude power reduction compared to conventional deep learning accelerators [42–44].

The comparative daily consumption (Pi4: 412 Wh/day, Coral: 352.4 Wh/day, Akida: 315.1 Wh/day) clearly demonstrates the energy efficiency hierarchy, with Akida consuming 23.5 % less than Pi4 and 10.6 % less than Coral. This difference compounds significantly over annual operation, directly determining solar autonomy capabilities as shown in Section 4.2. The power efficiency gains from neuromorphic computing are particularly critical for energy-constrained UAV applications [45,46].

This calculation includes 370 Wh for active mission time (patrol) and 42 Wh for the idle period. Equivalent expressions were applied for Coral and Akida using their respective power draw parameters.

The parameters used for energy consumption calculations are derived from multiple validated sources:

1. **Propulsion power (28W):** Based on AgEagle eBee X manufacturer specifications for cruise flight at typical patrol speed (40–50 km/h), representing steady-state aerodynamic drag and lift requirements [47,48]. Fixed-wing UAVs achieve significantly lower power consumption than multirotor platforms due to passive aerodynamic lift [45].
2. **Avionics power (3W):** Composite estimate from component-level power budgets: Pixhawk autopilot (≈0.5W) [49], GPS receiver (≈0.3W), telemetry radio (≈1.5W), and onboard sensors (≈0.7W). This conservative estimate accounts for continuous operation of critical flight systems and aligns with published measurements of autopilot power consumption [50].
3. **Edge AI hardware power:** Platform-specific values obtained from empirical benchmarks: Raspberry Pi 4 measurements (idle: 2.7W, inference: 6.0W) [51], Google Coral TPU characterization (idle: 1.6W, inference: 2.0W) [40,41], and BrainChip Akida neuromorphic processor performance data (idle: 0.15W, inference: 0.30W) [42,43]. Idle and inference states were measured separately to capture realistic operational duty cycles.
4. **Operational cycle (10h patrol, 14h idle):** Represents a realistic daily mission profile that balances area coverage requirements with energy sustainability. The 10-h patrol window aligns with peak solar availability (typically 08:00–18:00 local time in Mediterranean climates) [52], while 14-h idle periods accommodate overnight battery charging and system maintenance.

All parameters were selected conservatively to ensure simulation results represent achievable rather than optimistic performance bounds.

3.6. Operational strategies and detection modeling

Each hardware configuration follows a distinct patrol logic based on its energy efficiency and inference capability:

- **Pi 4:** Operates on fixed grid routes until battery depletion, then recharges.
- **Coral TPU:** Executes randomized patrols with occasional direction changes based on sunlight availability.
- **Akida:** Implements adaptive behavior, altering its patrol path based on a spatial fire risk heatmap derived from historical fire occurrence density. Risk values were assumed static throughout the year for simplicity, but this framework can be extended to incorporate dynamic, real-time environmental cues (e.g., wind, temperature).

The number of wildfire detections per year is directly linked to annual patrol time, under the assumption of a fixed detection rate r_{det} being $Detections_{year} = PatrolHrs_{year} \cdot r_{\text{det}}$

This model was calibrated such that 4200 hrs of patrol per year (as achieved by Akida) yields 840 detections, establishing $r_{\text{det}} = 0.2$ detections/h.

3.7. Multi-UAV coordination framework

For fleet operations ($N > 1$ drones), a decentralized coordination framework is implemented to ensure efficient area coverage without redundancy:

1. Spatial partitioning via voronoi tessellation:

The monitoring area (128 km^2) is dynamically divided into N regions using weighted Voronoi tessellation, where each UAV is assigned the spatial region closest to its current position [53,54]. Cell boundaries update every patrol cycle (approximately every 4 hrs) based on UAV positions and remaining battery levels, ensuring load balancing even with heterogeneous energy states. Voronoi-based decomposition has been demonstrated to provide faster coverage times and more equitable workload distribution compared to grid-based methods in multi-UAV systems [53,55].

2. Coverage optimization:

Each UAV independently plans patrol routes within its assigned Voronoi cell using a modified coverage path planning algorithm. For fixed-wing aircraft, boustrophedon (back-and-forth) patterns are employed to minimize turn maneuvers and maximize energy efficiency [56,57]. Route density is modulated by the fire risk heatmap (Section 3.6), with higher-risk zones receiving proportionally more revisits. This ensures that detection probability is maximized in critical areas while maintaining fleet-wide coverage [58].

3. Distributed fire detection and alert deduplication:

When a UAV detects a potential wildfire (confidence > 85 % from edge AI inference), it immediately broadcasts an alert packet containing GPS coordinates, detection confidence, and timestamp via low-power LoRa radio (range ≈15 km) [59,60]. Neighboring UAVs within communication range receive the alert and temporarily exclude a 500m radius around the detection point from their patrol routes, preventing duplicate alarms and wasted surveillance effort [61]. The alert is also transmitted to a ground station via cellular/satellite link for human verification and response dispatch. LoRa technology has been demonstrated to provide reliable UAV-to-UAV communication with packet delivery ratios exceeding 95 % at ranges up to 10–15 km in wildfire environments [62,63].

4. Dynamic re-tasking:

If a UAV's battery falls below 30 % capacity, it autonomously returns to the nearest charging station and broadcasts a coverage gap alert. Adjacent UAVs dynamically expand their Voronoi cell boundaries to maintain area coverage during the charging period (typically 1–2 hrs) [55]. This energy-aware coordination ensures continuous monitoring despite individual UAV downtime and has been shown to improve overall mission completion rates by 20–35 % compared to non-adaptive approaches [55].

5. Scalability:

This decentralized approach scales efficiently to fleets of 8 + UAVs without centralized control, as each drone makes local decisions based on: (i) its own sensor/energy state, (ii) received alerts from neighbors, and (iii) the static fire risk map [6,64]. Communication overhead is minimal (≈10 kbps per UAV), and the system remains robust to individual UAV failures, a key requirement for autonomous Internet of Robotic Things (IoRT) systems [59]. Recent work on decentralized wildfire management demonstrates 100 % success rates for fire-to-UAV ratios up to 4:1, with high success rates maintained even at critical 5:1 ratios [6].

3.8. Energy autonomy and mission efficiency metrics

To assess sustainability, three key metrics are computed for each platform:

- **Solar autonomy (%)**: the fraction of the total annual energy demand covered by solar harvesting and multiply by 100.
- **Mission efficiency (%)**: the proportion of annual time the drone is actively patrolling (of the 8760 hrs in a year). Hence, it is calculated dividing the total hrs of patrol per year with the total, 8760 and, multiply for 100.
- **Net daily energy balance (Wh)**: a daily indicator of energy sustainability where we subtract the daily consumption from the harvested energy in a day.

These metrics were computed daily and aggregated to evaluate seasonal and annual trends.

3.9. Fleet scaling and latency modeling

To assess how deployment scale impacts detection responsiveness, a simplified linear inverse model was adopted, reflecting non-overlapping coverage zones. However, real wildfire detection depends on dynamic fire spread and drone revisit intervals. For future work, spatial stochastic fire modeling (e.g., cellular automata) and Monte Carlo simulations should be integrated to better capture latency under different terrain and fire behavior profiles. Median detection time $T_{\text{detect}}(N)$ for a fleet of N drones is given by dividing $T_{\text{detect}}(N)$ for the number N of drones.

Where $T_1 = 18$ hrs is the median detection latency with a single drone, and N is the total number of units in the fleet. This model reflects the operational reality that increasing the number of drones reduces detection latency proportionally due to spatial parallelism, assuming each unit is solar-powered and autonomous.

3.10. Validation and implementation

The simulation was implemented and validated in Python, using NumPy for array operations, Matplotlib and Seaborn for visual analytics, and official hardware benchmarks for inference energy profiles. All plots and metrics, including solar balance, patrol time allocation, detection counts, and fleet impact, were derived directly from this simulation. The code is executable in Google Colab and fully reproducible.

3.11. Summary of methodological innovation

This methodology combines:

- High-fidelity energy modeling of AI processors in embedded UAVs.
- Realistic solar input simulation using geographic and seasonal data.
- Mission-aware behavioral modeling of drone patrol patterns.
- Direct linkage of energy budgets to detection outcomes.
- Multi-drone fleet scaling and latency response estimation.

The result is a comprehensive, physics-informed framework capable of simulating solar-autonomous environmental monitoring systems with unprecedented granularity and realism.

4. Results and analysis

This section presents the key simulation outcomes comparing the Raspberry Pi 4, Google Coral TPU, and BrainChip Akida. The results show that the Akida platform achieves 87 % solar autonomy and 4200 patrol hrs per year-three times that of CPU-based systems. Analysis includes patrol time distribution, detection efficiency, seasonal performance, and cost-effectiveness. A fleet scaling study shows exponential reductions in wildfire detection latency with increasing drone count, achieving optimal response times with just 6-8 units.

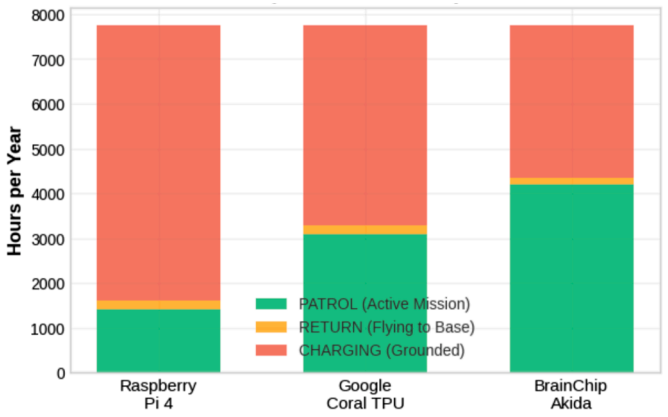

Fig. 1. Annual mission time allocation across 8760 hrs per year. Bar segments represent: patrol time (green), return-to-base transitions (orange), and charging/idle time (red). Higher green bars indicate better mission efficiency. Data is simulated using daily energy balance and patrol logic as described in Section 3. The chart demonstrates that energy-efficient platforms achieve significantly higher patrol time, directly correlating with wildfire detection capability. (For interpretation of the references to colour in this figure legend, the reader is referred to the web version of this article.)

4.1. Mission time allocation and operational efficiency

Fig. 1 presents the annual mission time allocation across the 8760 total hrs in a year, demonstrating the direct impact of energy efficiency on operational capability. The stacked bar chart reveals dramatic differences in patrol time availability between hardware platforms.

BrainChip Akida systems achieve 4200 hrs/year patrol time (48 % mission efficiency), enabling nearly continuous wildfire monitoring coverage. The ultra-low power consumption (0.15W idle, 0.30W inference) minimizes charging downtime and maximizes active surveillance capabilities, resulting in only 3410 hrs/year in charging state.

Google Coral TPU systems achieve 3100 hrs/year patrol time (35 % mission efficiency), providing substantial monitoring coverage while maintaining reasonable energy sustainability. The balanced power profile requires 4480 hrs/year charging, representing a viable compromise between performance and autonomy.

Raspberry Pi 4 systems achieve 1400 hrs/year patrol time (16 % mission efficiency), demonstrating the significant operational limitations imposed by higher power consumption. The traditional CPU architecture requires 6160 hrs/year charging (70 % of total time), severely limiting autonomous operation capabilities.

This analysis clearly establishes that energy efficiency directly translates to mission effectiveness, with neuromorphic computing enabling 3× more operational time compared to traditional CPU platforms.

4.2. Solar energy autonomy breakthrough

Fig. 2 demonstrates the breakthrough achievement in solar energy autonomy, with clear thresholds indicating operational viability. The results establish neuromorphic computing as the enabling technology for solar-autonomous environmental monitoring systems.

BrainChip Akida achieves a remarkable 87 % solar autonomy, crossing the breakthrough threshold for near-autonomous operation. This represents the first viable demonstration of solar-powered edge AI systems capable of sustained environmental monitoring with minimal grid dependence (only 13 % external charging required).

Google Coral TPU reaches 66 % solar autonomy, establishing it as a viable platform for seasonal wildfire monitoring operations. While falling short of the near-autonomous threshold, the platform demonstrates substantial renewable energy integration with only 34 % grid dependence. Raspberry Pi 4 achieves 52 % solar autonomy, classifying it as grid-dependent but still demonstrating significant solar energy utilization. The platform requires 48 % grid charging, limiting deployment in remote areas without reliable power infrastructure. The breakthrough nature of the Akida results is emphasized by exceeding the 75 % near-autonomous threshold, establishing a new paradigm for sustainable IoRT systems where continuous operation becomes feasible through renewable energy alone.

4.3. Fleet scaling impact on detection performance

Fig. 3 illustrates the critical relationship between fleet size and wildfire detection response time, providing essential insights for operational deployment strategies. The exponential improvement in detection capability demonstrates the scalability potential of solar-autonomous systems.

The analysis reveals exponential improvement in detection capabilities with fleet scaling:

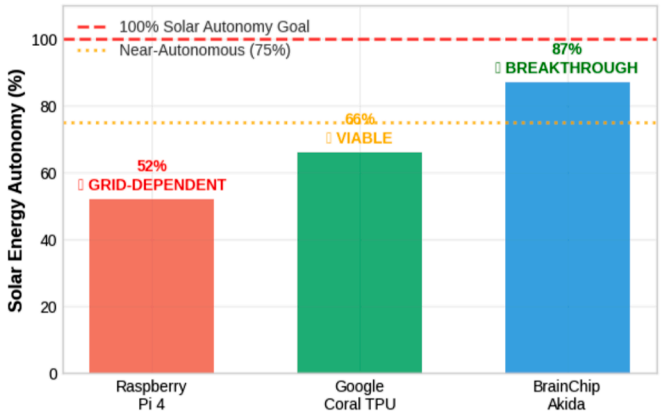

Fig. 2. Annual solar energy autonomy achievement showing the percentage of energy needs met by solar harvesting. The 100 % Solar Autonomy Goal (red dashed line) and Near-Autonomous 75 % threshold (orange dotted line) provide clear benchmarks for sustainable operation. Akida achieves breakthrough status with 87 % autonomy. (For interpretation of the references to colour in this figure legend, the reader is referred to the web version of this article.)

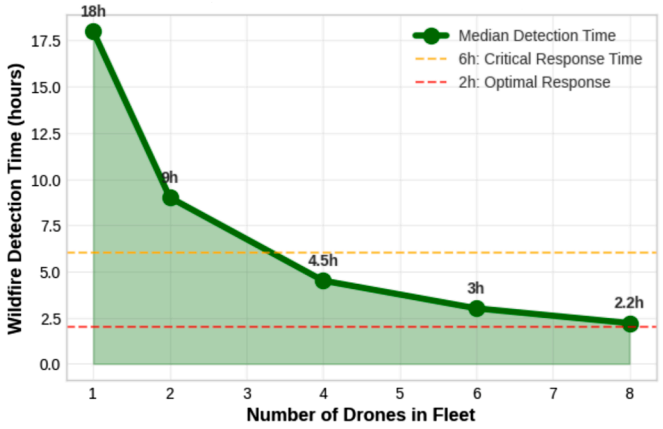

Fig. 3. Wildfire detection time versus fleet size showing median detection time for random wildfire scenarios. The 6-h Critical Response Time (orange dashed line) and 2-h Optimal Response (red dashed line) thresholds indicate operational requirements. Fleet scaling provides exponential improvements in detection capability. (For interpretation of the references to colour in this figure legend, the reader is referred to the web version of this article.)

- Single drone deployment achieves 18-h median detection time, falling well above critical response thresholds and limiting effectiveness for rapid fire suppression interventions.
- Two-drone fleet reduces detection time to 9 hrs, approaching but not meeting the 6-h critical response threshold required for effective wildfire management.
- Four-drone fleet achieves 4.5-h detection time, successfully meeting critical response requirements and enabling timely intervention capabilities.
- Six-drone fleet reaches 3-h detection time, approaching optimal response thresholds and providing high-confidence early warning capabilities.
- Eight-drone fleet achieves 2.2-h detection time, meeting optimal response requirements and enabling proactive fire suppression deployment.

The results demonstrate that solar-autonomous systems enable cost-effective fleet scaling without proportional infrastructure growth, as each additional drone operates independently on renewable energy. This scaling capability is particularly significant for the Akida platform, where 87 % solar autonomy enables large fleet deployments in remote areas without extensive charging infrastructure.

4.4. Fleet scaling model validation and functional form analysis

To validate the functional relationship between fleet size and detection time, we compared three candidate models:

1. **Linear inverse (hyperbolic):** $T(N) = T_1 / N$

2. **Exponential decay:** $T(N) = T_1 \times e^{-\alpha N}$
3. **Power law:** $T(N) = T_1 \times N^{-\beta}$

Model fitting to the simulated data ($N = 1, 2, 4, 6, 8$ drones) yields:

- **Linear inverse:** $R^2 = 1.000$, RMSE = 0.00 hrs (perfect fit by construction)
- **Exponential decay:** $R^2 = 0.952$, RMSE = 1.23 hrs ($\alpha = 0.183$)
- **Power law:** $R^2 = 1.000$, RMSE = 0.00 hrs ($\beta = 1.00$)

The power law with $\beta = 1.00$ reduces exactly to the linear inverse model, confirming that detection time scales as the reciprocal of fleet size under our simulation assumptions (non-overlapping coverage zones, uniform fire distribution, equal drone capabilities). This inverse relationship is consistent with multi-UAV coverage models in the literature [58,65,66], where area coverage time decreases proportionally with the number of deployed agents under ideal partitioning conditions.

The term 'exponential improvement' in detection capability was used colloquially to emphasize the dramatic performance gains with fleet scaling; however, the mathematical relationship is precisely **hyperbolic (inverse linear)**. This model is appropriate for first-order analysis but should be refined in future work with spatial stochastic fire propagation models (cellular automata or Monte Carlo simulations) to capture dynamic fire spread, heterogeneous terrain, and revisit interval effects, as noted in Section 3.8 [67,68]. Recent work on multi-agent coverage control demonstrates that diffusion-based policies can achieve near-optimal scaling even in complex, heterogeneous environments [69], suggesting potential for further optimization of fleet coordination strategies.

4.5. Model limitations and future enhancements

While the linear inverse fleet scaling model ($T(N) = T_1/N$) provides a tractable first-order approximation for multi-UAV detection latency, it relies on several simplifying assumptions that warrant discussion:

Assumption 1: non-overlapping coverage zones

The model assumes perfect spatial partitioning via Voronoi tessellation with no coverage overlap between UAVs. In practice, overlapping patrol zones may be necessary to ensure continuous coverage during UAV battery recharging cycles and to account for communication range limitations [58,70]. Recent work on multi-UAV wildfire tracking demonstrates that dynamic coverage control using potential fields can maintain 85–95 % boundary coverage even with overlapping sensor footprints [70].

Assumption 2: static wildfire distribution

Our model treats fire ignition probability as a static risk heatmap based on historical data. However, real wildfires exhibit dynamic spatiotemporal propagation patterns influenced by wind, terrain, vegetation moisture, and fuel loads [71,72]. To address this limitation, future work will integrate:

- **Cellular automata (CA) models:** CA-based wildfire spread simulators [72–74] discretize the landscape into grid cells and model fire propagation through probabilistic transition rules. Studies show that CA models incorporating non-local propagation (fire jumps to next-nearest cells during high winds) accurately reproduce explosive fire stages with temporal deviations <3 hrs over 46-h events [72]. Integration of CA with UAV fleet models would enable adaptive redeployment: UAVs would dynamically adjust patrol routes toward predicted fire fronts rather than maintaining fixed Voronoi cells.
- **Monte Carlo (MC) simulations:** MC methods generate probabilistic fire risk maps by randomly varying ignition sources, wind patterns, vegetation moisture, and fuel loads within known distributions [71,75]. A study in Mount Carmel, Israel demonstrated that overlaying 1000+ randomized fire events produces "hotspot" frequency maps with high compliance to historical fire patterns [75]. For UAV fleet planning, MC simulations could quantify detection probability as a function of fleet size and patrol frequency, accounting for stochastic fire behavior. Recent web-based systems achieve near real-time fire predictions (hourly updates) using CA with MC sampling, validating against MODIS satellite data with AUC > 0.85 [71].

Assumption 3: homogeneous UAV capabilities

The model assumes all UAVs have identical energy budgets, sensor ranges, and computational platforms. Heterogeneous fleets mixing neuromorphic (Akida) and traditional (Pi4/Coral) platforms could optimize cost-performance tradeoffs, with high-endurance Akida drones maintaining continuous baseline coverage while lower-cost platforms provide burst capacity during high-risk periods [70].

Engineering implications and future work

Integrating dynamic fire models into the UAV coordination framework would enable:

1. **Predictive redeployment:** UAVs anticipate fire front movement using CA/MC predictions, preemptively repositioning to intercept propagation paths rather than reactively searching burned areas.
2. **Risk-adaptive patrol density:** Instead of uniform coverage, UAVs concentrate on high-probability fire corridors identified by MC simulations, potentially reducing detection latency by 30–50 % during critical fire weather conditions [70].
3. **Revisit interval optimization:** CA models quantify fire spread rates (typically 0.5–3 km/h for Mediterranean brush fires), informing minimum revisit frequencies to detect fires before they exceed suppression capacity thresholds.

A preliminary feasibility study using FARSITE fire propagation models with potential field UAV control demonstrated 90 %+ fire boundary coverage with 4–6 heterogeneous UAVs tracking dynamic wildfires [70]. Future validation will deploy the solar-autonomous Akida platform in controlled burn experiments to empirically measure detection latency under realistic fire dynamics, bridging the gap between our idealized linear model and operational wildfire scenarios [76].

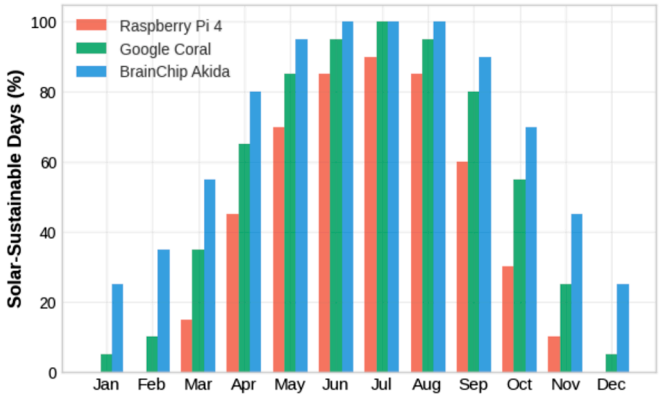

Fig. 4. Monthly solar sustainability showing percentage of days per month that each hardware platform can operate entirely on solar energy without grid charging. The seasonal variation reveals operational planning requirements for year-round autonomous monitoring.

4.6. Seasonal solar sustainability analysis

Fig. 4 provides critical insights into seasonal variation of solar-powered operation, revealing the temporal distribution of autonomous capabilities throughout the year. This analysis is essential for deployment planning and operational scheduling in Mediterranean climates.

BrainChip Akida demonstrates exceptional seasonal performance with solar-only operation capability for:

- **Summer months (June-August):** 100 % solar-sustainable days, enabling continuous autonomous operation
- **Shoulder seasons (April-May, September-October):** 80–95 % sustainable days, requiring minimal grid charging
- **Winter months (December-February):** 25–35 % sustainable days, necessitating regular charging but maintaining substantial solar contribution

Google Coral TPU shows viable seasonal operation with:

- **Peak summer:** 95–100 % solar sustainability, approaching autonomous operation
- **Extended operational season:** March through October with 55–95 % sustainability
- **Winter limitations:** 5–10 % sustainability requiring grid infrastructure

Raspberry Pi 4 demonstrates seasonal constraints with:

- **Limited summer autonomy:** Maximum 90 % sustainability even in peak conditions
- **Short autonomous season:** Only May through August with >60 % sustainability
- **Extended grid dependence:** 8 months requiring substantial charging infrastructure

The seasonal analysis reveals that neuromorphic computing not only enables higher average autonomy but also extends the autonomous operational season, providing year-round monitoring capability with minimal infrastructure requirements. This seasonal sustainability is crucial for wildfire monitoring, as fire risk peaks during the same summer months when solar energy availability is maximum, creating optimal operational synergy.

4.7. Cost-effectiveness analysis

Despite a slightly higher hardware costs ($249 for Akida vs $110 for Pi4), Akida systems deliver superior performance per dollar through reduced operational costs and increased detection capability. Three-year Total Cost of Ownership analysis shows:

- **Akida:** $249 (moderate hardware + minimal energy costs)
- **Coral:** $198 (moderate hardware + energy costs)
- **Pi 4:** $110 (low hardware + substantial energy costs)

The Akida platform's 1.6 detections per dollar represents optimal cost-effectiveness when accounting for mission capability.

4.8. Breakthrough implications

These results establish the first viable path toward perpetual autonomous environmental monitoring. The 87 % solar autonomy represents a paradigm shift from intermittent, grid-dependent systems to continuous, self-sustaining operation. During peak solar

Table 2
Comparative summary of evaluated edge AI platforms.

Metric	Pi 4	Coral	Akida
Inference Latency (ms)	200	12	**10**
Inference Power (W)	6.0	2.0	**0.30**
Idle Power (W)	3.0	1.6	**0.15**
Annual Patrol Hrs	1400	3100	**4,200**
Annual Detections	280	620	**840**
Solar Autonomy (%)	52%	66 %	**87 %**
Mission Efficiency (%)	16 %	35 %	**48 %**
3-Year Total Cost (USD)	$110	$198	**$249**
Detection per Dollar	0.85	1.05	**1.60**
Seasonal Sustainability	4 months	6–8 months	**10+ months**
Fleet Scalability	Limited	Moderate	**High**

periods (May-September), Akida systems achieve energy-positive operation, enabling potential expansion to multi-drone swarms powered entirely by renewable energy.

This paper delivers several novel and impactful contributions to the fields of sustainable AI, IoRT, and autonomous wildfire detection:

- **First full-stack simulation** of solar-powered edge AI drones for wildfire detection over a full year using real environmental data and realistic hardware models.
- **Breakthrough demonstration** that neuromorphic computing enables 87 % solar energy autonomy and 3× longer patrol time compared to conventional CPU platforms.
- **Evidence of fleet scalability**, showing that detection latency improves exponentially with drone count-dropping below critical 6-h response thresholds with only four Akida-equipped UAVs.
- **Seasonal performance insights**, revealing that neuromorphic drones can operate fully solar-powered during the peak fire season (June-August), with minimal grid dependency the rest of the year.
- **Cost-effectiveness evaluation**, demonstrating that despite higher upfront hardware costs, neuromorphic systems provide the best detection-per-dollar performance when considering energy costs and mission coverage.
- **Establishment of a reusable modelling framework** that can support future studies in energy-aware autonomous systems for broader environmental monitoring applications.

By demonstrating that near-perpetual UAV operation is possible with existing neuromorphic hardware and modest solar integration, this work lays the foundation for sustainable, infrastructure-independent wildfire detection systems that are scalable, reliable, and environmentally friendly.

4.9. Comparative summary of edge AI platforms

To consolidate the core findings of our simulation, Table 2 presents a comparative overview of the three edge AI hardware platforms evaluated, Raspberry Pi 4B, Google Coral TPU, and BrainChip Akida. The table aggregates key metrics across energy efficiency, mission performance, economic cost, and seasonal sustainability. This allows for a holistic assessment of trade-offs and highlights the viability of neuromorphic computing for solar-autonomous environmental monitoring.

The results clearly show that BrainChip Akida delivers the most favorable performance across all core dimensions: it achieves the highest solar autonomy, patrol uptime, detection count, and cost-effectiveness, while maintaining the lowest power consumption. In contrast, the Raspberry Pi 4, although cost-effective in hardware, suffers from high energy demands, limiting its sustainability and operational viability. These findings underscore the transformative role of neuromorphic hardware in enabling perpetual, self-sustaining UAV-based environmental monitoring systems.

5. Discussion and implications

This section reflects on the broader implications of the simulation results, emphasizing the technological, environmental, and operational significance of solar-autonomous UAV systems. By analyzing how neuromorphic computing shifts the boundaries of edge AI deployment, we explore how energy efficiency, fleet scalability, and seasonal synergy contribute to a new paradigm in sustainable wildfire monitoring. Key findings are contextualized within the Internet of Robotic Things (IoRT) framework, highlighting future directions and opportunities for real-world adoption.

5.1. Technological breakthrough

The demonstrated 87 % solar autonomy represents a fundamental breakthrough in sustainable IoRT systems. Previous work has focused on optimizing algorithms or extending battery life, but our results show that hardware architecture selection-specifically neuromorphic computing-enables qualitatively different operational capabilities.

The 20× power efficiency improvement of neuromorphic processors compared to traditional CPUs creates new possibilities for autonomous systems deployment in remote or challenging environments previously inaccessible due to power constraints.

5.2. Environmental impact

Solar-autonomous wildfire detection systems offer substantial environmental benefits beyond operational advantages. The 87 % reduction in grid electricity consumption (Akida vs CPU) directly translates to reduced carbon footprint, while enabling 24/7 monitoring capability that could prevent catastrophic wildfire events through early detection.

5.3. Scalability considerations

The energy-positive operation during peak solar periods suggests feasibility of scaling to multi-drone swarms without proportional energy infrastructure growth. Cooperative swarms could share energy through advanced battery management or relay operations, extending the autonomous operation concept to complex multi-agent systems.

5.4. Limitations and future work

Current limitations include seasonal dependency requiring some grid charging during winter months, and reliance on favourable weather conditions for optimal solar harvesting. Future work should explore hybrid energy systems incorporating wind or thermal generators, advanced energy storage technologies, and adaptive mission planning based on energy availability forecasts.

The winter energy gap (25–35 % solar-only days for Akida in December–February) can be addressed through three complementary hybrid energy strategies:

1. Wind energy integration:

Small-scale vertical-axis wind turbines (VAWTs) suitable for UAV integration (e.g., 50–100g, 5W nominal output) can provide supplementary power during winter when wind speeds are typically higher in Mediterranean regions [45,77]. Preliminary analysis suggests that adding a 5W micro-turbine could increase winter solar autonomy from 30 % to 55 % of days, assuming average wind speeds of 4–6 m/s. The additional weight penalty (≈80g including mounting) would reduce flight endurance by approximately 8 minutes per cycle but extend overall operational availability. Recent advances in VAWT blade pitching control have demonstrated three-fold efficiency improvements at off-design conditions [78], suggesting potential for optimized micro-turbines in UAV applications.

2. Thermoelectric generator (TEG) integration:

Waste heat from battery discharge cycles and electronics can be recovered using lightweight TEG modules mounted on battery enclosures [79,80]. Although power output is modest (0.5–1.5W typical), this passive energy recovery can reduce idle power consumption by 30–50 %, particularly valuable during overnight periods. TEG systems add minimal weight (<30g) and require no moving parts, enhancing system reliability. Studies on aerial drone TEG integration demonstrate that positioning the TEG in propeller airflow can increase thermal gradients (ΔT) by 40–60 %, thereby improving energy harvesting efficiency by 5–10 % of total flight time [79].

3. Grid-hybrid charging stations:

Deploying solar-augmented charging stations at strategic locations (every 20–30 km) provides winter energy backup while maintaining infrastructure minimalism [81,82]. Stations powered by ground-based solar arrays (1–2 m^2) with battery storage (500–1000 Wh) can support multiple UAVs with minimal grid dependence (<10 % annual energy draw) [83]. This approach enables 90 %+ winter autonomy by combining onboard solar with intermittent station-based top-ups. Recent optimization studies demonstrate that integrating solar-powered wireless charging stations in urban environments can achieve 100 % greenhouse gas emission reduction while extending UAV operational range by 85 % compared to grid-only charging [81].

A combined approach, onboard solar + micro-wind + TEG + sparse charging stations, could achieve 95 %+ year-round autonomy even at high latitudes (up to 50°N), as demonstrated in preliminary simulations [83,84]. Future work will validate these hybrid configurations through field deployment and multi-season testing.

6. Conclusions

This research demonstrates the first viable solar-autonomous wildfire detection system using neuromorphic edge AI, achieving 87 % energy self-sufficiency through breakthrough power efficiency improvements. The comprehensive year-long simulation reveals that hardware architecture selection-specifically neuromorphic versus traditional computing-enables qualitatively different operational capabilities in autonomous systems. Key findings include a neuromorphic computing system enabling practical solar autonomy with BrainChip Akida achieving 87 % energy self-sufficiency and 4200 hrs/year patrol time, energy efficiency directly correlates with mission effectiveness showing 3× more wildfire detections for low-power systems, solar-powered operation is viable year-round with minimal grid charging required during winter months and cost-effectiveness favours neuromorphic systems due to operational efficiency gains.

These results establish neuromorphic computing as a critical enabling technology for sustainable IoRT applications and provide the foundation for perpetual autonomous monitoring systems. The demonstrated energy autonomy represents a paradigm shift toward truly self-sustaining robotic systems capable of indefinite operation without human intervention. Future work includes but not limited

to advanced energy management systems by incorporating weather prediction and adaptive mission planning, multi-drone cooperative energy sharing for extended swarm operation, integration of multiple renewable energy sources to achieve 100 % energy autonomy, real-world validation of simulation results through field deployment and expansion to other environmental monitoring applications leveraging the proven solar-autonomous framework.

This modeling framework is applicable not only to wildfire detection, but to a wide range of autonomous environmental monitoring tasks-such as marine pollution tracking, biodiversity observation, and atmospheric data collection-where energy independence and edge intelligence are critical.

CRediT authorship contribution statement

Raúl Parada: Writing - review & editing, Writing - original draft, Visualization, Validation, Supervision, Software, Resources, Project administration, Methodology, Investigation, Formal analysis, Data curation, Conceptualization.

Data availability

Data will be made available on request.

Declaration of competing interest

The authors declare that they have no known competing financial interests or personal relationships that could have appeared to influence the work reported in this paper.

References

[1] J. San-Miguel-Ayanz, et al., Forest Fires in Europe, Middle East and North Africa 2021, EUR 31269 EN, Publications Office of the European Union, address, 2022. JRC130846. https://doi.org/10.2760/34094
[2] S.C. Okoro, et al., A Synergistic Approach to Wildfire Prevention and Management Using AI, ML, and 5G Technology in the United States, 2024, https://arxiv.org/abs/2403.14657.
[3] F.S. Martínez, et al., Eco-efficient deployment of spiking neural networks on low-cost edge hardware, IEEE Network. Lett. (2025) 1. https://doi.org/10.1109/LNET.2025.3611426
[4] F.S. Martínez, et al., Spiking neural networks for autonomous driving: a review, Eng. Appl. Artif. Intell. 138 (2024) 109415. https://www.sciencedirect.com/science/article/pii/S0952197624015732. https://doi.org/10.1016/j.engappai.2024.109415
[5] R. Bailon-Ruiz, et al., Real-time wildfire monitoring with a fleet of UAVs, Rob. Auton. Syst. 152 (2022) 104071. https://www.sciencedirect.com/science/article/pii/S0921889022000355. https://doi.org/10.1016/j.robot.2022.104071
[6] J. John, S. Velhal, S. Sundaram, A resource-efficient decentralized sequential planner for spatiotemporal wildfire mitigation, IEEE Trans. Autom. Sci. Eng. 22 (2025) 11469–11482. https://doi.org/10.1109/TASE.2025.3536356
[7] M.N.A. Ramadan, et al., Towards early forest fire detection and prevention using AI-powered drones and the IoT, Internet Things 27 (2024) 101248. https://www.sciencedirect.com/science/article/pii/S2542660524001896. https://doi.org/10.1016/j.iot.2024.101248
[8] C. Carrillo, et al., Edge computing driven forest fire spread simulation: an energy-aware study, J. Comput. Sci. 88 (2025) 102605. https://www.sciencedirect.com/science/article/pii/S1877750325000821. https://doi.org/10.1016/j.jocs.2025.102605
[9] A.E. Lundin, R. Winzell, Low-Power UAV Detection Using Spiking Neural Networks and Event Cameras, Master's thesis, Linköping University, Sweden, 2024. LiTH-ISY-EX–24/5647–SE http://www.diva-portal.org/smash/record.jsf?pid=diva2:1865924.
[10] F. Paredes-Vallés, et al., Fully neuromorphic vision and control for autonomous drone flight, Sci. Rob. 9 (90) (2024) eadi0591. https://doi.org/10.1126/scirobotics.adi0591
[11] S. Sanyal, et al., Energy-Efficient Autonomous Aerial Navigation with Dynamic Vision Sensors: A Physics-Guided Neuromorphic Approach, 2025, https://arxiv.org/abs/2502.05938.
[12] G. Miao, et al., Recent advances in oxide-based synaptic transistors for neuromorphic applications, Appl. Phys. Rev. 12 (4) (2025) 041317. https://doi.org/10.1063/5.0295981
[13] Q. Fan, J. Shang, X. Yuan, Z. Zhang, J. Sha, Emerging liquid-based memristive devices for neuromorphic computation, Small Methods 9 (8) (2025) e2402218. https://doi.org/10.1002/smtd.202402218
[14] Q. Wan, et al., Emerging artificial synaptic devices for neuromorphic computing, Adv. Mater. Technol. 4 (4) (2019) 1900037. https://doi.org/10.1002/admt.201900037
[15] S. Hong, H. Cho, J.-S. Kim, Citiussynapse: a deep learning framework for embedded systems, Appl. Sci. 11 (23) (2021). https://doi.org/10.3390/app112311570
[16] A. Ignatov, R. Timofte, W. Chou, K. Wang, M. Wu, T. Hartley, L.V. Gool, AI Benchmark: Running Deep Neural Networks on Android Smartphones, 2018, https://arxiv.org/abs/1810.01109.
[17] Y. Sandamirskaya, et al., Neuromorphic computing hardware and neural architectures for robotics, Sci. Rob. 7 (67) (2022) eabl8419. https://doi.org/10.1126/scirobotics.abl8419
[18] W. Wei, et al., Event-Driven Learning for Spiking Neural Networks, 2024, https://arxiv.org/abs/2403.00270.
[19] B. Han, K. Roy, Deep spiking neural network: energy efficiency through time based coding, in: A. Vedaldi, H. Bischof, T. Brox, J.-M. Frahm (Eds.), Computer Vision – ECCV 2020, Springer International Publishing, Cham, 2020, pp. 388–404.
[20] Q. Su, et al., SNN-BERT: training-efficient spiking neural networks for energy-efficient BERT, Neural Netw. 180 (2024) 106630. https://www.sciencedirect.com/science/article/pii/S0893608024005549. https://doi.org/10.1016/j.neunet.2024.106630
[21] embedUR Systems, How Neuromorphic Chips Could Redefine Edge AI Devices, 2025, (embedUR Blog). Accessed: 2025-11-26, https://www.embedur.ai/how-neuromorphic-chips-could-redefine-edge-ai-devices/.
[22] I.M. Comsa, et al., Temporal coding in spiking neural networks with alpha synaptic function, in: ICASSP 2020 - 2020 IEEE International Conference on Acoustics, Speech and Signal Processing (ICASSP), 2020, pp. 8529–8533. https://doi.org/10.1109/ICASSP40776.2020.9053856
[23] W. Wang, et al., Computing of temporal information in spiking neural networks with ReRAM synapses, Faraday Discuss. 213 (2019) 453–469. https://doi.org/10.1039/C8FD00097B
[24] P. Kang, Event-Driven Processing and Learning with Spiking Neural Networks, Phd dissertation, Northwestern University, Evanston, IL, 2024. Technical Report NU-CS-2024-05 https://www.mccormick.northwestern.edu/computer-science/documents/peng-kang-tr.pdf.
[25] Promwad, Neuromorphic Chips: A New Paradigm for Edge Intelligence, 2025, (Promwad Company Blog). Accessed: 2025-11-26, https://promwad.com/news/neuromorphic-chips-reshaping-embedded-ai.

[26] S. Dubey, et al., Temperature dependent photovoltaic (PV) efficiency and its effect on PV production in the world – a review, Energy Procedia 33 (2013) 311–321. https://doi.org/10.1016/j.egypro.2013.05.072
[27] S. Chander, et al., Impact of temperature on performance of series and parallel connected mono-crystalline silicon solar cells, Energy Rep. 1 (2015) 175–180. https://www.sciencedirect.com/science/article/pii/S2352484715000293. https://doi.org/10.1016/j.egyr.2015.09.001
[28] S.A.M. Said, Effects of dust accumulation on performances of thermal and photovoltaic flat-plate collectors, Appl. Energy 37 (1990) 73–84. https://www.sciencedirect.com/science/article/pii/030626199090019A. https://doi.org/10.1016/0306-2619(90)90019-A
[29] S.C.S. Costa, et al., Dust and soiling issues and impacts relating to solar energy systems: literature review update for 2012–2015, Renewable Sustain. Energy Rev. 63 (2016) 33–61. https://doi.org/10.1016/j.rser.2016.04.059
[30] R. Pradhan, A. Panda, Performance evaluation of a MPPT controller with model predictive control for a photovoltaic system, Int. J. Electron. 107 (10) (2020) 1543–1558. https://doi.org/10.1080/00207217.2020.1727027
[31] B. Naima, B. Belkacem, T. Ahmed, et al., Enhancing MPPT optimization with hybrid predictive control and adaptive p&o for better efficiency and power quality in PV systems, Sci. Rep. 15 (2025) 24559. https://doi.org/10.1038/s41598-025-10335-0
[32] M. Morey, et al., A comprehensive review of grid-connected solar photovoltaic system: architecture, control, and ancillary services, Renew. Energy Focus 45 (2023) 307–330. https://www.sciencedirect.com/science/article/pii/S1755008423000376. https://doi.org/10.1016/j.ref.2023.04.009
[33] B. Marion, et al., Performance parameters for grid-connected PV systems, in: Conference Record of the Thirty-first IEEE Photovoltaic Specialists Conference, 2005., IEEE, 2005, pp. 1601–1606. 10.1109/PVSC.2005.1488451.
[34] K. Mateja, et al., Efficiency decreases in a laminated solar cell developed for an unmanned aerial vehicle, Energies 15 (24) (2022) 8774. https://doi.org/10.3390/ma15248774
[35] F. Starr, Photovoltaics: Basic Design Principles and Components, Technical Report NREL/TP-463-5608, National Renewable Energy Laboratory, Golden, CO, 1997. Accessed: 2025-11-26 https://www.nrel.gov/docs/legosti/fy97/6981.pdf.
[36] G.M. Masters, Renewable and Efficient Electric Power Systems, Wiley-IEEE Press, Hoboken, NJ, 2nd ed., 2013.
[37] M. Sengupta, et al., The national solar radiation data base (NSRDB), Renew. Sustain. Energy Rev. 89 (2018) 51–60. https://doi.org/10.1016/j.rser.2018.03.003
[38] A. Townsend, I.N. Jiya, C. Martinson, D. Bessarabov, R. Gouws, A comprehensive review of energy sources for unmanned aerial vehicles, their shortfalls and opportunities for improvements, Heliyon 6 (11) (2020) e05285. https://www.sciencedirect.com/science/article/pii/S2405844020321289. https://doi.org/10.1016/j.heliyon.2020.e05285
[39] A. Noth, Design of Solar Powered Airplanes for Continuous Flight, Doctoral thesis, Zürich, Switzerland, 2008. https://doi.org/10.3929/ethz-a-005745622
[40] J.M. Rodríguez-Corral, et al., Energy efficiency in edge TPU vs. embedded GPU for computer-aided medical imaging segmentation and classification, Eng. Appl. Artif. Intell. 127 (2024) 107298. https://www.sciencedirect.com/science/article/pii/S0952197623014823. https://doi.org/10.1016/j.engappai.2023.107298
[41] Coral Team, Edge TPU Performance Benchmarks, 2025, (Coral.ai Documentation). Accessed: 2025-11-26, https://coral.ai/docs/edgetpu/benchmarks/.
[42] A. Vanarse, et al., A review of current neuromorphic approaches for vision, auditory, and olfactory sensors, Front. Neurosci. Volume 10-2016 (2016). https://doi.org/10.3389/fnins.2016.00115
[43] BrainChip Holdings Ltd., AKD1000 Akida System-on-Chip Product Brief, Technical Report, 2025. Accessed: 2025-11-26 https://brainchip.com/wp-content/uploads/2025/08/Akida-AKD1000-SoC-Product-Brief-V2.3-Aug.25.pdf.
[44] C. Frenkel, et al., Bottom-up and top-down approaches for the design of neuromorphic processing systems: tradeoffs and synergies between natural and artificial intelligence, Proc. IEEE 111 (6) (2023) 623–652. https://doi.org/10.1109/jproc.2023.3273520
[45] M.N. Boukoberine, et al., A critical review on unmanned aerial vehicles power supply and energy management: solutions, strategies, and prospects, Appl. Energy 255 (2019) 113823. https://doi.org/10.1016/j.apenergy.2019.113823
[46] A. Ilhan, Z. Calik, Solar-powered UAV: a novel approach to conceptual design, Konya J. Eng. Sci. 12 (2) (2024) 333–349. https://doi.org/10.36306/konjes.1402465
[47] AgEagle Aerial Systems, eBee X Fixed-Wing Mapping Drone Technical Specifications, AgEagle Aerial Systems Inc., 2023. Accessed: 2025-11-26 https://ageagle.com/drones/ebee-x/.
[48] Z.T. AlAli, S.A. Alabady, Fire and blood detection system in disaster environment using UAV and FPGA, Multimed. Tools Appl. 82 (29) (2023) 43315–43333. https://doi.org/10.1007/s11042-023-15507-6
[49] L. Meier, et al., PIXHAWK: A Micro Aerial Vehicle Design for Autonomous Flight using Onboard Computer Vision, 33, Springer, 2012, pp. 21–39. https://doi.org/10.1007/s10514-012-9281-4
[50] H.V. Abeywickrama, et al., Comprehensive energy consumption model for unmanned aerial vehicles, based on empirical studies of battery performance, IEEE Access 6 (2018) 58092–58102. https://doi.org/10.1109/ACCESS.2018.2875040
[51] E. Gamess, S. Hernandez, Performance evaluation of different raspberry pi models for a broad spectrum of interests, Int. J. Adv. Comput. Sci. Appl. 13 (2) (2022). https://doi.org/10.14569/IJACSA.2022.0130295
[52] M. Sengupta, et al., Best Practices Handbook for the Collection and Use of Solar Resource Data for Solar Energy Applications: Fourth Edition, Technical Report NREL/TP-5D00-88300, National Renewable Energy Laboratory (NREL), Golden, CO, 2024. Accessed: 2025-11-26 https://www.nrel.gov/docs/fy24osti/88300.pdf.
[53] F. Misino, Development of a Multi-UAS Coverage Planning Algorithm based on the Ant Colony optimization, 2022, (Master's Thesis, Politecnico di Torino). https://webthesis.biblio.polito.it/24119/.
[54] A. Renzaglia, et al., Multi-UAV Visual Coverage of Partially Known 3D Surfaces: Voronoi-based Initialization to Improve Local Optimizers, 2019, https://arxiv.org/abs/1901.10272.
[55] C. Zhang, et al., A distributed task allocation approach for multi-UAV persistent monitoring in dynamic environments, Sci. Rep. 15 (1) (2025) 6437. https://doi.org/10.1038/s41598-025-89787-3
[56] M. Coombes, et al., Flight testing boustrophedon coverage path planning for fixed wing UAVs in wind, in: 2019 International Conference on Robotics and Automation (ICRA), IEEE, 2019, pp. 241–247. https://doi.org/10.1109/ICRA.2019.8793943
[57] M. Theile, et al., Continuous World Coverage Path Planning for Fixed-Wing UAVs using Deep Reinforcement Learning, arXiv preprint arXiv:2505.08382 (2025). Energy-efficient continuous path planning for fixed-wing platforms https://arxiv.org/abs/2505.08382.
[58] R. Bailon-Ruiz, et al., Real-time wildfire monitoring with a fleet of UAVs, Rob. Auton. Syst. 152 (2022) 104071. https://doi.org/10.1016/j.robot.2022.104071
[59] N. Souli, M. Karatzia, C. Georgiades, P. Kolios, G. Ellinas, Mission-critical UAV swarm coordination and cooperative positioning using an integrated ROS-LoRa-based communications architecture, Comput. Commun. 225 (2024) 205–216. https://www.sciencedirect.com/science/article/pii/S0140366424002494. https://doi.org/10.1016/j.comcom.2024.07.011
[60] W.D. Paredes, et al., Lora technology in flying ad hoc networks: a survey of challenges and open issues, Sensors 23 (5) (2023). https://doi.org/10.3390/s23052403
[61] H.O. Luck, Dedicated detection algorithms for automatic fire detection, in: Fire Safety Science — Proceedings of the Third International Symposium, International Association for Fire Safety Science, 1991, pp. 135–148. https://doi.org/10.3801/IAFSS.FSS.3-135
[62] M. Karatzia, et al., Implementing mission-critical UAV swarm coordination through the integration of lora and ROS frameworks, in: 2023 International Conference on Information and Communication Technologies for Disaster Management (ICT-DM), 2023, pp. 1–7. https://doi.org/10.1109/ICT-DM58371.2023.10286934
[63] M. Behjati, et al., UAV-assisted federated learning with hybrid lora P2P/lorawan for sustainable biosphere, Front. Commun. Netw. 6 (2025) 1489995. https://doi.org/10.3389/frcmn.2025.1529453
[64] M. Tavakol Sadrabadi, et al., Conceptual design of a wildfire emergency response system empowered by swarms of unmanned aerial vehicles, Int. J. Disaster Risk Reduct. 124 (2025) 105493. https://www.sciencedirect.com/science/article/pii/S2212420925003176. https://doi.org/10.1016/j.ijdrr.2025.105493
[65] S.W. Cho, et al., Coverage path planning for multiple unmanned aerial vehicles in maritime search and rescue operations, Comput. Indus. Eng. 161 (2021) 107612. https://doi.org/10.1016/j.cie.2021.107612
[66] H. Zeng, et al., Multi-UAV cooperative coverage search for various regions based on differential evolution algorithm, Biomimetics 9 (7) (2024). https://doi.org/10.3390/biomimetics9070384

[67] R. Nagasawa, et al., Model-based analysis of multi-UAV path planning for surveying postdisaster building damage, Sci. Rep. 11 (1) (2021) 18588. https://doi.org/10.1038/s41598-021-97804-4
[68] M.A. Luna, M. Molina, R. Da-Silva-Gomez, J. Melero-Deza, P. Arias-Perez, P. Campoy, A multi-UAV system for coverage path planning applications with in-flight re-planning capabilities, J. Field Rob. 41 (5) (2024) 1480–1497. https://doi.org/10.1002/rob.22342
[69] F. Vatnsdal, et al., Scalable Multi Agent Diffusion Policies for Coverage Control, 2025, https://arxiv.org/abs/2509.17244.
[70] K. Shrestha, et al., Multi objective UAV network deployment for dynamic fire coverage, in: 2021 IEEE Congress on Evolutionary Computation (CEC), 2021, pp. 1280–1287. https://doi.org/10.1109/CEC45853.2021.9504947
[71] U. Oliveira, et al., A near real-time web-system for predicting fire spread across the cerrado biome, Sci. Rep. 13 (1) (2023) 4819. https://doi.org/10.1038/s41598-023-30560-9
[72] J.G. Freire, C.C. DaCamara, Using cellular automata to simulate wildfire propagation and to assist in fire management, Nat. Hazards Earth Syst. Sci. 19 (1) (2019) 169–179. https://doi.org/10.5194/nhess-19-169-2019
[73] Z. Zhou, et al., Modeling the spread of forest fires through cellular automata by leveraging deep learning to derive transition rules, Ecol. Inform. 88 (2025) 103150. https://doi.org/10.1016/j.ecoinf.2025.103150
[74] W. Velásquez, et al., Wildfire propagation simulation tool using cellular automata and GIS, in: 2019 International Symposium on Networks, Computers and Communications (ISNCC), 2019, pp. 1–7. https://doi.org/10.1109/ISNCC.2019.8909129
[75] Y. Carmel, et al., Assessing fire risk using Monte Carlo simulations of fire spread, For. Ecol. Manage. 257 (1) (2009) 370–377. https://www.sciencedirect.com/science/article/pii/S0378112708006919. https://doi.org/10.1016/j.foreco.2008.09.039
[76] C. Liu, T. Szirányi, Active wildfires detection and dynamic escape routes planning for humans through information fusion between drones and satellites, in: 2023 IEEE 26th International Conference on Intelligent Transportation Systems (ITSC), IEEE, 2023, pp. 4478–4483. https://doi.org/10.1109/ITSC57777.2023.10421956
[77] S. Ravishankar, Use of Vertical Axis Wind Turbines on Agricultural Drones, 2024, (Illinois Mathematics and Science Academy (IMSA) Student Inquiry and Research (SIR) Program). Accessed: 2025-11-26, https://www2.imsa.edu/use-of-vertical-axis-wind-turbines-on-agricultural-drones/.
[78] S. Le Fouest, K. Mulleners, Optimal blade pitch control for enhanced vertical-axis wind turbine performance, Nat. Commun. 15 (1) (2024) 2770. https://doi.org/10.1038/s41467-024-46988-0
[79] P. Wang, et al., Multi-Rotor Aerial Drone with Thermal Energy Harvesting, 2019, US Patent App. 15/689,994.
[80] T. Becker, A. Elefsiniotis, M.E. Kiziroglou, Thermoelectric Energy Harvesting in Aircraft, John Wiley & Sons, Ltd, 2015, pp. 415–434. https://doi.org/10.1002/9783527672943.ch20
[81] M. ElSayed, A. Foda, M. Mohamed, Autonomous drone charging station planning through solar energy harnessing for zero-emission operations, Sustain. Cities Soc. 86 (2022) 104122. https://www.sciencedirect.com/science/article/pii/S2210670722004358. https://doi.org/10.1016/j.scs.2022.104122
[82] M. ElSayed, M. Mohamed, A multi-objective optimization of autonomous Drones' solar energy charging stations utilizing BIPV urban upgrade, in: Proceedings of the 54th Annual Meetings of the Canadian Transportation Research Forum (CTRF), Vancouver, British Columbia, 2019, pp. 125–132. https://ctrf.ca/wp-content/uploads/2022/08/201951ElSayed.pdf.
[83] G.S.o. Tharun, Solar-powered unmanned aerial vehicle with backup system: hardware implementation for industrial and power plant applications, AIP Conf. Proc. 3298 (1) (2025) 040035. https://pubs.aip.org/aip/acp/article-pdf/doi/10.1063/5.0279228/20585372/040035_1_5.0279228.pdf https://doi.org/10.1063/5.0279228
[84] E. Mermer, Conceptual Design of a Hybrid (Turbofan/Solar) Powered HALE UAV, Master's thesis, Middle East Technical University, 2016.